Advanced Ceramics Progress: Vol. 11, No. 4, (Autumn 2025) 21-30

Materials and Energy Research Center
MERC

Contents lists available at ACERP

Advanced Ceramics Progress

Journal Homepage: www.acerp.ir

Original Research Article

A Comparative Study of Microstructure and Mechanical Properties in Copper Processed by Simple Shear Extrusion and Elliptical Cross-Section Spiral Equal-Channel Extrusion

Mostafa Balali[a, *]

[a] Instructor, Department of Mechanical Engineering, Hakim Sabzevari University, Sabzevar, Iran.

* Corresponding Author Email: balalimostafa@outlook.com (M. Balali)

URL: https://www.acerp.ir/article_247020.html

ARTICLE INFO

Article History:

Received 08 June 2026
Revised 17 June 2026
Accepted 05 July 2026

Keywords:

Severe Plastic Deformation
Simple Shear Extrusion
Elliptical Cross-Section Spiral Equal Channel Extrusion
Mechanical Properties
Microstructural Properties

ABSTRACT

One of the well-known approaches for producing ultrafine-grained and nanostructured materials is severe plastic deformation (SPD), which has attracted significant attention in recent years. This study investigates the microstructural evolution and mechanical properties of commercially pure copper processed by two SPD methods: Simple Shear Extrusion (SSE) and Spiral Equal-Channel Extrusion with an Elliptical Cross-Section (ECSEE). Samples underwent four sequential extrusion passes at room temperature using both techniques and were subsequently characterized through metallography, microhardness measurements, tensile testing, and forming force analysis. The results demonstrate a substantial enhancement in mechanical properties and grain refinement with each additional pass for both processes. However, the ECSEE method, which imposes more severe plastic strain, yielded superior results. Specifically, after four passes, the ECSEE-processed samples achieved an ultimate tensile strength of 349 MPa and a microhardness of 166 HV, representing increases of 104% and 9%, respectively, compared to the annealed condition. In contrast, the SSE method, which applies lower and more gradual strain, resulted in an ultimate tensile strength of 242 MPa and a microhardness of 139 HV after four passes. Microstructural analysis revealed reductions in grain size of 28% and 17% for the ECSEE- and SSE-processed samples, respectively, after the fourth pass. Furthermore, the SSE method required a lower forming force due to the lower strain imposed. The findings conclusively indicate that the ECSEE process produces superior microstructural characteristics and enhanced mechanical behavior, including strength, microhardness, and ductility, compared to the SSE method.

https://doi.org/10.30501/acp.2026.584598.1197

1. INTRODUCTION

In recent years, bulk nanostructured materials (NSMs) produced through severe plastic deformation (SPD) techniques have drawn growing interest among materials science researchers (Valiev., 1996). Drawing operations at low temperatures can bring about a considerable enhancement of the microstructure (Haasen., 1996; Sevillano et al., 1980). However, the resulting structures are typically cellular, with boundaries containing low-angle dislocations. In contrast, the nanostructures produced by SPD are ultrafine-grained structures consisting mainly of grains with high-angle grain boundaries. Achieving such nanostructures is possible

Please cite this article as: Balali, M. (2025). A Comparative Study of Microstructure and Mechanical Properties in Copper Processed by Simple Shear Extrusion and Elliptical Cross-Section Spiral Equal-Channel Extrusion. *Advanced Ceramics Progress*, *11*(4), 21-30. https://doi.org/10.30501/acp.2026.584598.1197

through SPD methods, which impose large strains at relatively low temperatures and under high pressures (Valiev et al., 1993; Valiev et al., 1998). These methods can simultaneously yield a suitable combination of strength and ductility, whereas other methods often result in increased strength at the expense of reduced ductility (Tsuji et al., 2002). Materials produced by SPD are of great interest because of their high strength and toughness. Notable SPD processes include equal-channel angular pressing (ECAP), simple shear extrusion (SSE), accumulative roll bonding (ARB), high-pressure torsion (HPT), and multi-axial forging (MAF) (Valiev et al., 2006). Pardis and Ebrahimi (Pardis and Ebrahimi., 2009) invented and introduced the SSE process in 2009. The SSE technique was proposed as an innovative approach to address a key limitation of the conventional ECAP method, specifically its substantial material waste. SSE enables the production of high-strength materials through grain refinement while preserving the original dimensions of the workpiece without significant alteration. In this process, samples are pressed longitudinally through a straight channel with a specific profile. The sample cross-section changes from a square at the channel inlet to a parallelogram, reaching its maximum shear angle at the midpoint, before returning to a square at the outlet (Balali et al., 2018; Balali et al., 2021). Tork et al. (Tork et al., 2013) explored the feasibility of achieving plastic deformation in pure magnesium at room temperature through the SSE technique. Their findings revealed that specimens subjected to ECAP, constrained angle dropping (CAD), and double equal-channel lateral extrusion (DECLE) deteriorated as a result of localized shear strain. In contrast, the samples processed by SSE remained largely intact. Bagherpour et al. (Bagherpour et al., 2016) studied the extrusion of commercially pure copper samples via the SSE process. They showed that, in addition to grain refinement, the hardness of the material increased significantly.

Wang et al. (Wang et al., 2013) invented and introduced the elliptical cross-section spiral equal-channel extrusion (ECSEE) process in 2013. In this method, the cross-section of a cylindrical sample is circular at the channel entrance, deforms into an elliptical shape in the plastic deformation zone, and finally exits the channel as a circle. As one of the SPD methods, the ECSEE process can impose significant strain on the material, leading to improved mechanical properties and the production of ultrafine-grained materials (Wang et al., 2018; Latypov et al., 2013). According to Mills et al. (Mills et al., 2025) the application of ECAP leads to a substantial improvement in the mechanical performance of zinc. This enhancement is attributed to the effective refinement of the material's microstructure. Following four ECAP passes, the grain size is reduced by more than half, while the yield strength increases by up to 80%. The choice of deformation route critically influences both microstructural uniformity and processability, with Route BC providing the most consistent grain refinement and strengthening, while Route C proved the most viable by producing crack-free billets for subsequent applications.

Through the development of a novel Mg-Sn-Zn-Zr alloy and the application of an innovative differential thermal equal-channel angular pressing (DT-ECAP) method, Zhou et al. (Zhou et al., 2024) successfully addressed the strength-ductility trade-off typically observed in magnesium alloys. The developed material exhibited an outstanding balance of properties, including an ultimate tensile strength of approximately 340-370 MPa and considerable ductility (approximately 27-33% elongation). These improvements were achieved through grain refinement, ultrafine precipitates, and the activation of multiple dislocation slip systems that promoted superior work hardening.

In their study, Ge et al. (Ge et al., 2024) developed Mg-Zn-Mn alloys by integrating zinc additions with an innovative SPD method known as screw twist extrusion (STE). This approach resulted in refined grain structures and improved ductility. The STE process generates a gradient microstructure, weakens the texture, and refines grains through twist-induced strain, while the formation of $MgZn_2$ phases resulting from high Zn content further promotes dynamic recrystallization (DRX) through continuous dynamic recrystallization (CDRX), discontinuous dynamic recrystallization (DDRX), and particle-stimulated nucleation (PSN) mechanisms. Consequently, the synergistic effect of Zn alloying and STE significantly increases the Schmid factor for basal slip, leading to a remarkable improvement in fracture elongation from 18.4% to 27.8%, demonstrating an effective strategy for enhancing ductility in Mg-Zn-Mn alloys.

Balali et al. (Balali et al., 2025) proposed a hybrid technique that integrates ultrasonic vibrations into the SSE process for pure copper, with vibrations applied precisely at the entry of the deformation zone. To deliver these oscillations, the authors developed a specially designed horn with a cylindrical-conical-cylindrical geometry, optimized using modal analysis in Abaqus software. This horn operates at a resonant frequency of 20.332 kHz and is capable of generating amplitudes of 15 µm and 25 µm. The results indicated an increase in microhardness due to acoustic hardening. Furthermore, the required extrusion force decreased because of acoustic softening, while finite element simulations confirmed enhanced and more uniform plastic strain distribution.

The extrusion of pure magnesium samples at 200 °C using the ECSEE method was successfully performed in another study. Observations indicated that after two extrusion passes, a fine grain size of 2.1 µm was achieved, and the strength of pure magnesium increased markedly to approximately 180 MPa, although its ductility decreased by about 12% (Li et al., 2021).

Given the above, the present research aims to investigate the evolution of the microstructure, the formation of a fine-grained structure, and the improvement in the strength and hardness of copper subjected to the SSE and ECSEE processes, as well as to compare their performance. The mechanical properties and microstructural characteristics obtained through standard specimens and laboratory testing are examined and discussed to evaluate the performance of the two processes.

2. MATERIALS AND METHODS

2.1. Design and Fabrication of the SSE and ECSEE Dies

To conduct the experimental tests, it was necessary to fabricate a die with high strength and crack resistance. During the initial fabrication of the SSE die, factors such as inappropriate material selection (SPK steel), improper heat treatment, and a two-piece design caused the die to crack under the applied press load. To address this issue, the SSE die was modeled using CATIA software and subsequently imported into Abaqus/Explicit for finite element simulation. Based on the simulation results, MO40 steel was selected as the die material. Finally, a controlled heat treatment process was applied to the die, resulting in a hardness of 54 HRC. A punch is required for sample extrusion. Based on preliminary investigations, SPK steel was selected for the punch to prevent buckling under the high press load. The punch was also fabricated to be compatible with the connection to the upper section of the press (the press ram). Figure 1 illustrates the SSE die. In the SSE process, commercially pure copper specimens with a square cross-section of 14 mm × 14 mm and a length of 50 mm were used. To facilitate extrusion and eliminate possible defects, the copper specimens were annealed at 610 °C for 2 h. Table 1 presents the chemical composition of the samples. The design and fabrication of the ECSEE die were carried out in a manner similar to that used for the SSE process, employing CATIA and Abaqus/Explicit software. Subsequently, the ECSEE dies were manufactured using milling, turning, and drilling operations, as shown in Figure 2. For the ECSEE method, specimens with a length of 60 mm were fabricated based on an input channel diameter of 15 mm.

Figure 1. A view of the SSE die

Figure 2. A view of the ECSEE die

TABLE 1. Chemical profile of the copper samples used in the SSE and ECSEE processes.

Element	Wt%
Cu	99.9
Ca	0.0001
Ag	0.0016
Pb	0.0008
P	0.0005
S	0.001
Fe	0.0012
Others	Bal.

2-2. Experimental Procedure of the SSE and ECSEE Methods

The universal press machine used for specimen extrusion had a capacity of 60 tons and featured an adjustable ram speed. In the SSE process, all specimens were prepared according to the specified dimensions. To perform the process, the specimens were lubricated with oil and placed into the inlet channel of the die. The die assembly was then positioned on the press table, and the punch was connected to the press ram through a sleeve. The pressing operation was initiated at a speed of 5 mm/min, and the specimens were subsequently driven through the die channel by the punch load. The experimental setup is illustrated in Figure 3.

After a complete extrusion stroke, the punch was retracted, and the next specimen was placed behind the previous one to continue the extrusion cycle. Throughout the process, the pressing speed was maintained constant to allow the specimen to exit the channel gradually and to prevent punch buckling. It is important to note that the punch position had to be adjusted carefully to avoid contact with the walls of the inlet channel during pressing, thereby preventing damage to the die.

The extrusion procedure in the ECSEE process, using identical spiral channels with an elliptical cross-section, was performed similarly to that of the SSE process. The key difference was that the specimens were cylindrical and underwent plastic deformation in the deformation zone of the die, where they were transformed into an elliptical shape. To ensure a consistent comparison between the SSE and ECSEE methods, the number of extrusion passes was set to four for both processes. Figure 4 illustrates the experimental procedure and sample extrusion by the ECSEE process. Figure 5 shows the deformation of the specimens within the plastic deformation zone for the SSE and ECSEE methods.

The experimental program was conducted separately for the SSE and ECSEE methods through consecutive passes. Specifically, the first pass consisted of one extrusion, the second pass of two extrusions, the third pass of three extrusions, and the fourth pass of four extrusions. In total, 10 separate extrusion trials were performed for each method, resulting in 20 trials overall. To compare and analyze the mechanical and microstructural properties of the SSE and ECSEE methods, metallographic, hardness, and tensile tests were conducted. For metallographic examination, the specimens were sectioned transversely and subjected to final polishing using a polishing machine and diamond paste. Subsequently, to reveal the grain structure, an etchant with a composition of 20 mL H_2O, 10 mL HCl, and 10 g $FeCl_3$ was prepared according to the ASM Handbook. The microstructural examination of the specimens was carried out using the linear intercept method in accordance with the ASTM E112 standard and analyzed using ImageJ software.

Furthermore, the microhardness of the specimens was measured on the front surface using a Shimadzu Vickers hardness tester under a load of 50 g applied for 20 s. To determine the yield strength and ultimate tensile strength, tensile specimens were prepared and tested under uniaxial loading in accordance with the ASTM E8 standard at a crosshead speed of 10 mm/min.

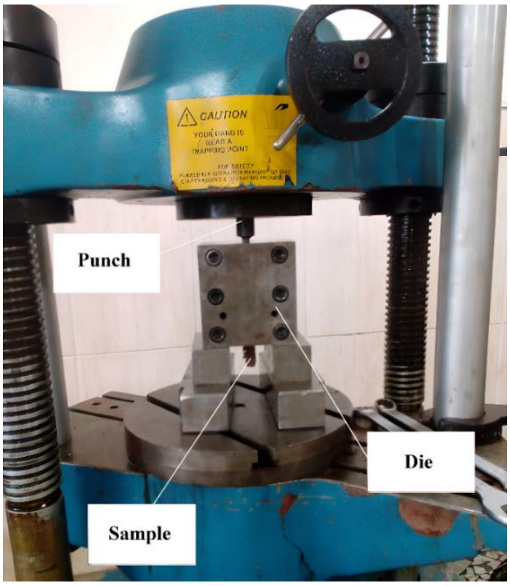

Figure 3. The extruding operation in the SSE process

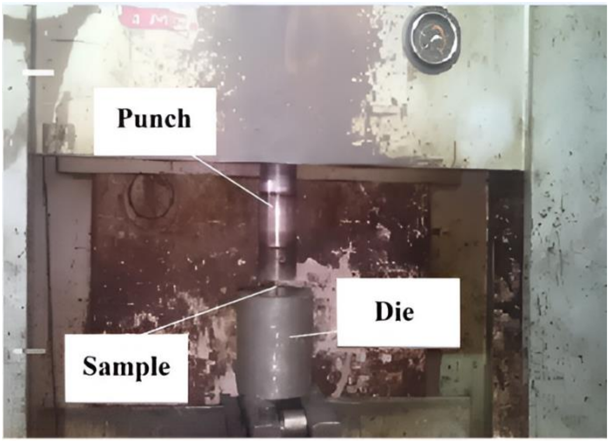

Figure 4. The extruding operation in the ECSEE process

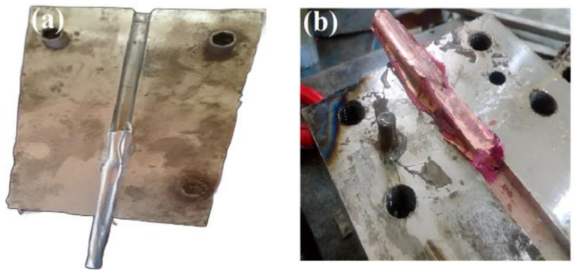

Figure 5. Variations in the (a) ECSEE-processed and (b) SSE-processed samples within the plastic deformation zone.

3. RESULTS AND DISCUSSION

3. 1. Comparison of the Forming Force Variations in the SSE and ECSEE Methods

The experimental forming force of the SSE process was extracted as a function of press ram displacement. The forming force refers to the load applied by the press machine through the punch to the specimen. This force acts as the driving mechanism that propels the specimen through the die channel and facilitates its passage through the deformation zone, ultimately resulting in plastic deformation of the material. Figure 6 shows the force-displacement curves of the SSE process for the four samples. As can be seen in Figure 6, in the SSE method, the material exhibits an increase in mechanical strength with increasing pass number, requiring greater force for sample extrusion. The forming force results indicated lower values for the first- and fourth-pass SSE samples compared with the corresponding ECSEE samples. This reduction in forming force can be attributed to energy absorption by dislocations and a decrease in the friction coefficient between the specimen and the die channel (Faraji et al., 2018). Since the strain imposed in the SSE process is lower than that in the ECSEE method, the punch load required for sample extrusion is correspondingly lower, making the extrusion process easier.

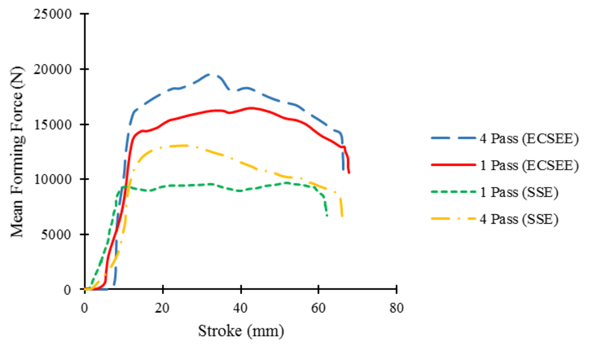

Figure 6. Force-Displacement Diagram in the SSE and ECSEE Methods

3.2. Examination and Comparison of the Microstructure of Extruded Samples in the SSE and ECSEE Processes

Figure 7 displays optical micrographs illustrating the microstructure of copper specimens after four passes of the SSE process. The mean grain dimensions, specifically the length and width, were calculated using MIP4 software to determine the average grain size. The initial microstructure of the homogenized and annealed sample exhibited an average grain size of 85 µm. Following the first pass, the microstructure underwent progressive refinement, becoming markedly different from the initial structure.

The microstructural evolution across the samples reveals a clear progression. Sample (a) exhibits relatively coarse and equiaxed α-Cu grains. In Sample (b), the structure becomes elongated and oriented, with insoluble precipitates and particles accumulating along the material flow direction. Sample (c) demonstrates a transition toward a more uniform and finer-grained α-Cu structure with a reduced presence of precipitates. Finally, Sample (d) displays a very fine-grained α-Cu structure characterized by a dispersion of fine intermetallic particles, indicative of pronounced work hardening.

The application of severe plastic deformation and very high strains significantly increases the dislocation density within the material. These dislocations tend to accumulate in an organized manner inside the grains, forming boundary structures. Initially, these boundaries are low-angle grain boundaries (LAGBs). With continued deformation, the low-angle boundaries progressively accumulate additional dislocations and eventually evolve into high-angle grain boundaries (HAGBs). This process is known as grain boundary rotation or boundary multiplication (El-Danaf et al., 2007). This mechanism is repeated within the grains until their size is sufficiently reduced, causing the newly formed grains to rotate. As the sample enters the die and passes through the deformation zone, dislocations begin to move until cell boundaries are formed. With an increasing number of passes, the low-angle boundaries progressively transform into high-angle boundaries, leading to further grain refinement (Salishchev et al., 1995).

As evident in Figure 8, the samples processed by the ECSEE method and subjected to a higher number of passes exhibited a finer microstructure. In this method, due to the application of higher strains, the grain size after the fourth pass was reduced by 28% compared to that of the annealed sample. The presence of high hydrostatic pressure coupled with intense shear strain generates a high density of crystal defects, particularly dislocations within the lattice, which are influential factors in grain refinement (Hosseini et al., 2009).

When a material is subjected to severe simple shear through SPD methods, a large number of dislocations are generated and multiplied. This results in a sharp increase in dislocation density, which serves as the primary mechanism responsible for the initial work hardening and strength enhancement. At low to moderate strains (e.g., after one to two passes), the high density of dislocations becomes entangled and rearranges into low-energy configurations, forming cell walls and subgrain boundaries. This marks the onset of grain refinement.

With increasing strain, the continued accumulation and rearrangement of dislocations cause the subgrain boundaries to absorb additional dislocations, gradually transforming them into HAGBs. This process effectively produces an ultrafine-grained (UFG) or nanostructured material. At very high strains, a balance is often reached between the generation of new dislocations and their annihilation through dynamic recovery. Consequently, the dislocation density within the grain interiors reaches a saturation level or may even decrease slightly, while the grain boundaries remain stable. The resulting microstructure consists of fine equiaxed grains with a relatively low internal dislocation density, contributing to improved thermal stability (Janeček et al., 2012; Gubicza et al., 2006).

The average grain size was determined using MIP4 image analysis software. For each condition, at least 200 grains were randomly selected from high-quality optical micrographs. The longest and shortest diameters of each grain (length and width) were measured manually with the assistance of the software's automatic boundary detection capability, and the average of these two values was considered the individual grain size. The final reported value represents the mean of all measured grains, ensuring statistical reliability.

In both the ECSEE and SSE processes, a significant reduction in grain size was observed up to the fourth pass. In the SSE process, the average grain size after the fourth pass was 3 µm, corresponding to a 17% reduction compared with that of the annealed sample. In the ECSEE process, due to the application of higher strains than in the SSE process, the grains exhibited less intergranular spacing. The combined effects of shear strain through the specimen thickness and the strain induced by the extrusion force along its axis led to a substantial increase in the total effective strain imposed on the samples. The SSE process also enables the production of specimens with high accumulated strain through multiple extrusion passes, ultimately resulting in very fine grain sizes.

Furthermore, twinning was observed in the microstructure of the SSE-processed samples. These twins act as barriers to dislocation motion, and their accumulation reduces the spacing between slip bands, thereby contributing to strengthening. According to the results, the ECSEE process produced more pronounced microstructural changes in samples subjected to higher strains, generated a greater dislocation density, and consequently resulted in more significant grain refinement than the SSE method.

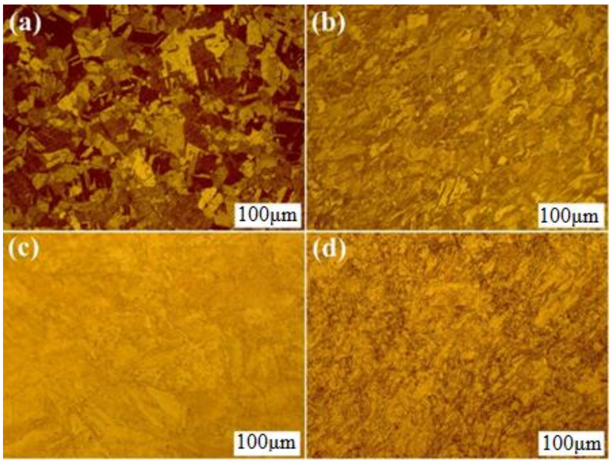

Figure 7. Optical microscopy images of the SSE specimens: (a) annealed condition; (b) single pass; (c) three passes; (d) four passes.

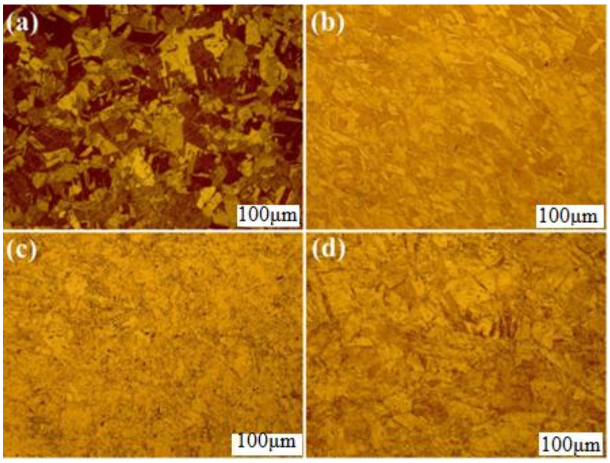

Figure 8. Optical microscopy images of the ECSEE specimens: (a) annealed condition; (b) single pass; (c) three passes; (d) four passes.

3.3. Investigation and Comparison of the Tensile Test in the SSE and ECSEE Processes

As evident in Figure 9, the tensile properties of the samples processed by the SSE method differ from one pass to another. After the first forming pass, the yield strength and ultimate tensile strength of the samples increased significantly, while their ductility and elongation decreased substantially. As an intrinsic material property, Young's modulus is not affected by mechanical processing such as strain hardening, including extrusion, rolling, or drawing. Consequently, its value remains essentially constant for both soft (annealed) and hard (cold-worked) copper. The parameters altered by these processes are the yield strength and ultimate tensile strength (Courtney., 2000). The reported yield strength values of the samples extruded by the SSE method after the first, third, and fourth passes were 149, 153, and 198 MPa, respectively. Similarly, the ultimate tensile strength values after the same passes were 168, 192, and 242 MPa, respectively. Comparison of the yield strength values of the extruded samples with that of the annealed sample indicates increases of 65%, 68%, and 79%, respectively. As the grain size decreases, the density of grain boundaries per unit volume increases significantly. These grain boundaries act as barriers that hinder dislocation motion and slip. According to the Hall-Petch relationship, grain refinement improves certain mechanical properties, such as yield strength, as expressed by Equation (1):

$$\sigma_y = \sigma_0 + Kd^{-\frac{1}{2}} \quad (1)$$

Where σy is the yield strength, d is the average grain diameter, σ0 is the lattice friction stress resisting the dislocation motion, and K is a material constant (Hall., 1951). This equation indicates an inverse relationship between yield strength and grain size; therefore, a decrease in grain size leads to an increase in yield strength. The accumulation of dislocations creates stress concentration regions at grain boundaries, which play a fundamental role in activating dislocation sources in adjacent grains and facilitating dislocation transfer. Consequently, a smaller grain size restricts such accumulation and limits the distribution of dislocations throughout the material volume. However, this mechanism is generally applicable only down to the nanometer scale. For grain sizes smaller than approximately 20 nm, the Hall-Petch relationship may no longer remain valid because other deformation mechanisms, such as grain boundary sliding, become dominant (Abenojar et al., 2008). The pronounced change in strain-rate sensitivity observed after three SSE passes may indicate a transition from dislocation-dominated slip to grain-boundary-mediated plasticity before microstructural saturation occurs after the fourth pass. This behavior has been reported in ultrafine-grained materials, where the competition between dislocation glide and diffusion-assisted mechanisms influences the rate dependence of plastic deformation. As a result, additional passes in the SSE process do not substantially modify the mechanical properties, since the material approaches a saturation state.

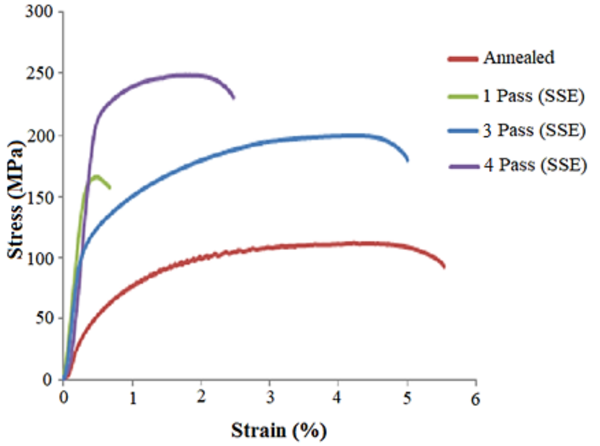

Figure 9. Stress-strain curve of copper processed by the SSE method

Figure 10 illustrates the stress-strain behavior of copper specimens subjected to different passes of the ECSEE process. A critical observation can be made from this figure. Unlike Figure 9, where lower total strains (up to approximately 5.5%) captured the transient nonequilibrium stage of grain refinement, Figure 10 represents substantially higher imposed strains, allowing the microstructure to reach a more saturated and stable ultrafine-grained state with equilibrated grain boundaries. In this regime, deformation is accommodated more uniformly by grain-boundary-mediated mechanisms, including grain boundary sliding and diffusion-assisted processes, resulting in a more stable flow behavior. Consequently, no abrupt change in strain-rate sensitivity is observed in Figure 10, suggesting that the pronounced transition observed in Figure 9 is associated primarily with the earlier stages of severe plastic deformation. Following the initial stages of the ECSEE process, the yield strength of the specimens increased significantly. As the process continued and the number of extrusion passes increased, the improvement in yield strength became more pronounced. According to Figure 10, the yield strength and ultimate tensile strength after the fourth pass increased by 262% and 104%, respectively, indicating a substantially greater improvement than that achieved by the SSE method. In both the SSE and ECSEE methods, strain hardening through dislocation generation and grain refinement are the primary mechanisms responsible for strength enhancement. The samples processed by the ECSEE method exhibited finer grain sizes than those processed by the SSE method, which explains the higher strength values obtained for the ECSEE-processed copper specimens.

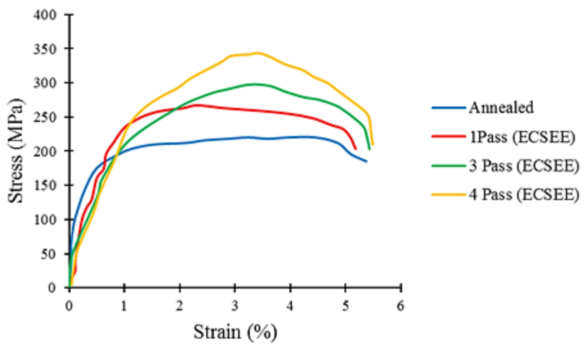

Figure 10. Stress-strain curve of copper processed by the ECSEE method

3.4. Microhardness Results of Copper Processed by the SSE and ECSEE Methods

Microhardness testing was performed on the frontal section and along the major diameter of the extruded samples. The corresponding results are presented in Figures 11 and 12. The hardness of the samples processed by both the SSE and ECSEE methods was higher than that of the annealed sample, which can be attributed to work hardening induced by severe plastic deformation.

The average microhardness values for the first to fourth passes of the SSE method were measured as 82, 111, 121, and 135 HV, respectively. For the ECSEE method, the corresponding values were 103, 134, 157, and 166 HV, respectively. Comparison of the average microhardness values at equivalent passes reveals an approximately 19% superiority of the ECSEE method over the SSE method. Notably, the hardness achieved after the second pass of the ECSEE method was comparable to that obtained after the fourth pass of the SSE method. The increase in hardness observed in both methods can be attributed primarily to the increased dislocation density within the material's microstructure (El-Danaf., 2008).

Strain hardening, also known as work hardening, is a fundamental metallurgical phenomenon in which a ductile metal exhibits enhanced strength and hardness as a result of plastic deformation. This strengthening mechanism originates from the complex interactions and multiplication of dislocations within the crystalline lattice. As plastic deformation progresses, dislocations become entangled and form pile-ups at microstructural barriers such as grain boundaries and other dislocations, thereby restricting further dislocation motion. The resulting resistance to dislocation movement manifests macroscopically as increased yield strength and hardness. In conventional deformation processes, this hardening mechanism typically reaches a saturation level before the onset of necking and eventual ductile fracture (Valiev et al., 2000).

To assess the uniformity of stress distribution across the deformed samples, systematic microhardness mapping using Vickers indentation was performed along both the longitudinal and transverse cross-sections with a step size of 0.5 mm, generating two-dimensional plots that visually reveal any strain gradients.

Furthermore, in the higher passes of both extrusion processes, the expected increase in hardness associated with grain refinement became less pronounced. This behavior can be attributed to the establishment of a stable dislocation density resulting from a dynamic balance between dislocation generation during severe plastic deformation and dislocation annihilation through dynamic recovery. Nevertheless, the overall trend in microhardness remained increasing throughout the SSE and ECSEE processes.

As shown in Figures 11 and 12, the microhardness at the center of the sample was higher than that in the surrounding regions due to the higher strains imposed in this area. The primary reasons for this behavior are strain hardening, grain refinement, and the formation of numerous barriers to dislocation motion.

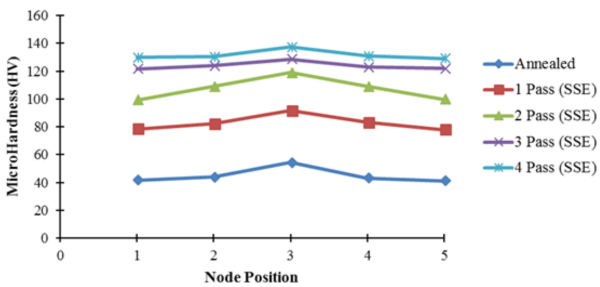

Figure 11. Microhardness results of the SSE-processed copper samples

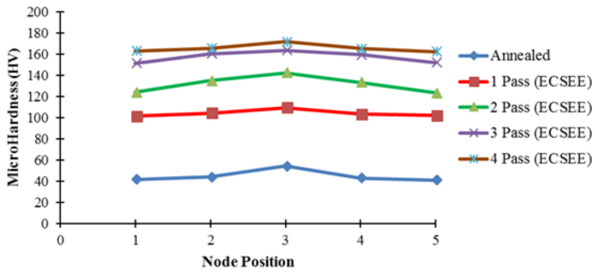

Figure 12. Microhardness results of the ECSEE-processed copper samples

4. CONCLUSION(S)

In the present study, copper samples were successfully processed using the SSE and ECSEE methods for up to four passes. To investigate and compare the mechanical and microstructural properties of the two processes, the samples were subjected to metallographic examination, microhardness testing, forming force measurements, and tensile testing. The main findings are summarized as follows:

- In the ECSEE method, the application of severe plastic strain resulted in a more pronounced improvement in the mechanical properties of the samples. In contrast, the SSE samples, due to the more gradual introduction of strain, exhibited a lower degree of strain hardening than the ECSEE samples.
- The SSE-processed samples exhibited lower strength and hardness than the ECSEE-processed samples at equivalent pass numbers. However, because strain is imposed more uniformly in the SSE method, a more homogeneous strain distribution was achieved along the length of the sample and across its frontal section, resulting in more uniform microstructural modification.
- The magnitude of the applied strain plays an important role in determining the forming force. Consequently, the SSE method, which imposes lower strain levels than the ECSEE method, required a lower forming force at equivalent pass numbers.
- The results obtained from the SSE process indicate that grain refinement led to simultaneous increases in strength and microhardness. The ultimate tensile strength increased from 58 MPa in the annealed condition to 242 MPa after four passes. Similarly, the average microhardness increased from 46 HV in the annealed condition to 139 HV after four passes. Furthermore, the processed samples exhibited no significant change in cross-sectional area.
- The results of the SSE and ECSEE processes showed that the grain size after the fourth pass was reduced by 17% and 28%, respectively, compared with that of the annealed sample. For the ECSEE samples, the

ultimate tensile strength and average microhardness after the fourth pass reached 349 MPa and 166 HV, respectively, representing increases of 104% and 9% relative to the annealed condition.

In terms of microstructural characteristics and mechanical performance, including strength, microhardness, and ductility, the samples processed by the ECSEE method exhibited superior properties compared with those processed by the SSE method.

NOMENCLATURE

SPD	Severe plastic deformation
SSE	Simple Shear Extrusion
ECSEE	Elliptical Cross-Section Spiral Equal-Channel Extrusion
NSMs	Nanostructured Materials
ECAP	Equal-Channel Angular Pressing
ARB	Cumulative Roll Bonding
HPT	High-Pressure Torsion
MAF	Multi-Axial Forging
CAD	Constrained Angle Dropping
DECLE	Double Equal Channel Lateral Extrusion
DT-ECAP	Differential Thermal Equal-Channel Angular Pressing
STE	Screw Twist Extrusion
USSE	Ultrasonic-Assisted Simple Shear Extrusion
LAGBs	Low-Angle Grain Boundaries
HAGBs	High-Angle Grain Boundaries
σy	Yield Strength
σ_0	Lattice Friction Stress
K	Material Constant
d	Average Grain Diameter

REFERENCES

1. Abenojar, J., Velasco, F., & Martínez, M. A. (2008). Optimization of processing parameters for the Al–10% B4C system obtained by mechanical alloying. *Journal of Materials Processing Technology, 328*(1–2), 222–229. 10.1016/j.jmatprotec.2006.11.122

2. Bagherpour, E., Pardis, N., Reihanian, M., & Ebrahimi, R. (2016). Microstructure quantification of ultrafine-grained pure copper fabricated by simple shear extrusion (SSE) technique. *Materials Science and Engineering: A, 674*, 221–231. https://doi.org/10.1016/j.msea.2016.08.001

3. Balali, M., Beynaghi, M., & Khosravi, M. (2021). Investigation of simple shear extrusion steel mold and mechanical properties of nanostructured extruded samples of Al6061. *International Journal of Iron and Steel Society of Iran, 18*(1), 106–112. 10.22034/ijissi.2021.540568.1211

4. Balali, M., Limouei, M. B., & Balali, M. (2018). Study on optimization of parameters affecting simple shear extrusion of pure copper to fabricate fine-grain structure. *Transactions of the Indian Institute of Metals, 71*(3), 605–616. https://doi.org/10.1007/s12666-017-1193-8

5. Balali,M , Seyedkashi,S M H , Hasanabadi,A , Gorji,H , Baseri,H and Khosravi,M . (2025). A New Ultrasonic-assisted Simple Shear Extrusion Process in Production of Ultrafine Grained Copper. International Journal of Engineering, 38(4), 908-920. 10.5829/ije.2025.38.04a.19

6. Courtney, T. H. (2000). *Mechanical behavior of materials* (2nd ed., pp. 85–87). Waveland Press.

7. El-Danaf, E. A. (2008). Mechanical properties and microstructure evolution of 1050 aluminum severely deformed by ECAP to 16 passes. *Materials Science and Engineering: A, 487*(1–2), 189–200. https://doi.org/10.1016/j.msea.2007.10.013

8. El-Danaf, E. A., Soliman, M. S., Almajid, A. A., & El-Rayes, M. M. (2007). Enhancement of mechanical properties and grain size refinement of commercial purity aluminum 1050 processed by ECAP. *Materials Science and Engineering: A, 458*(1–2), 226–234. https://doi.org/10.1016/j.msea.2006.12.077

9. Faraji, G., Kim, H. S., & Torabzadeh Kashi, H. (2018). *Severe plastic deformation: Methods, processing and properties*. Elsevier. 0128135670, 9780128135679

10. Ge, Z., et al. (2024). Effect of Zn addition combined with a novel screw twist extrusion technology on the microstructure, texture as well as the ductility of Mg-xZn-1Mn alloys. *Journal of Alloys and Compounds, 984*, 173995. https://doi.org/10.1016/j.jallcom.2024.173995

11. Gubicza, J., Chinh, N. Q., Krállics, G., Schiller, I., & Ungár, T. (2006). Microstructure of ultrafine-grained FCC metals produced by severe plastic deformation. *Current Applied Physics, 6*(2), 194–199. https://doi.org/10.1016/j.cap.2005.07.039

12. Haasen, P. (1996). Physical metallurgy. Cambridge university press.

13. Hall, E. O. (1951). The deformation and ageing of mild steel: III. Discussion of results. *Proceedings of the Physical Society Section B, 64*(9), 747–753. 10.1088/0370-1301/64/9/303

14. Hosseini, S. A., & Manesh, H. D. (2009). High-strength, high-conductivity ultra-fine grain commercial pure copper produced by the ARB process. *Materials & Design, 30*(8), 2911–2918. https://doi.org/10.1016/j.matdes.2009.01.012

15. Janeček, M., Čížek, J., Gubicza, J., & Vrátná, J. (2012). Microstructure and dislocation density evolutions in MgAlZn alloy processed by severe plastic deformation. *Journal of Materials Science, 47*(22), 7860–7869. https://doi.org/10.1007/s10853-012-6538-4

16. Latypov, M. I., Beygelzimer, Y., & Kim, H. S. (2013). Comparative analysis of two twist-based SPD processes: Elliptical cross-section spiral equal-channel extrusion vs. twist extrusion. *Materials Transactions, 54*(9), 1587–1591. https://doi.org/10.2320/matertrans.MH201315

17. Li, J., Wang, C., Li, F., & Liu, J. (2021). Microstructure and mechanical properties of pure Mg after spiral equal-channel extrusion. *Materials Science and Technology, 37*(4), 384–394. https://doi.org/10.1080/02670836.2021.1901366

18. Mills, K., Li, H., Luzin, V., & Kent, D. (2025). Influence of ECAP deformation routes on grain refinement, mechanical properties and texture of zinc. Materials Science and Engineering: A, 149066. https://doi.org/10.1016/j.msea.2025.149066

19. Pardis, N., & Ebrahimi, R. (2009). Deformation behavior in simple shear extrusion (SSE) as a new severe plastic deformation technique. *Materials Science and Engineering: A, 527*(1–2), 355–360. https://doi.org/10.1016/j.msea.2009.08.051

20. Salishchev, G. A., Zaripova, R. G., Galeev, R. M., & Valiakhmetov, R. (1995). Nanocrystalline structure formation during severe plastic deformation in metals and their deformation behavior. *Nanostructured Materials, 6*(5–8), 913–916. https://doi.org/10.1016/0965-9773(95)00208-1

21. Sevillano, J. G., Van Houtte, P., & Aernoudt, E. (1980). Large strain work hardening and textures. Progress in materials science, 25(2-4), 69-134. https://doi.org/10.1016/0079-6425(80)90001-8

22. Tork, N. B., Pardis, N., & Ebrahimi, R. (2013). Investigation on the feasibility of room temperature plastic deformation of pure magnesium by simple shear extrusion process. *Materials Science and Engineering: A, 560*, 34–39. https://doi.org/10.1016/j.msea.2012.08.085

23. Tsuji, N., Ito, Y., Saito, Y., & Minamino, Y. (2002). Strength and ductility of ultrafine-grained aluminum and iron produced by ARB and annealing. *Scripta Materialia, 47*(12), 893–899. 10.1016/S1359-6462(02)00282-8

24. Valiev, R. Z. (Ed.). (1996). *Ultra-fine-grained materials prepared by severe plastic deformation*. Annales de Chimie Science des Matériaux, 21, 369.

25. Valiev, R. Z., Alexandrov, I. V., & Islamgaliev, R. K. (1998). Nanocrystalline materials: Science and technology. In G. M. Chow & N. I. Noskova (Eds.), *NATO ASI Series* (p. 121). Kluwer Academic Publishers.

26. Valiev, R. Z., Islamgaliev, R. K., & Alexandrov, I. V. (2000). Bulk nanostructured materials from severe plastic deformation. *Progress in Materials Science, 45*(2), 103–189. https://doi.org/10.1016/S0079-6425(99)00007-9

27. Valiev, R. Z., Korznikov, A. V., & Mulyukov, R. R. (1993). Structure and properties of ultrafine-grained materials produced by severe plastic deformation. *Materials Science and Engineering: A, 168*(2), 141–148. https://doi.org/10.1016/0921-5093(93)90717-S

28. Valiev, R. Z., & Langdon, T. G. (2006). Principles of equal-channel angular pressing as a processing tool for grain refinement. *Progress in Materials Science, 51*(7), 881–981. https://doi.org/10.1016/j.pmatsci.2006.02.003

29. Wang, C., Li, F., Liu, J., & Li, J. (2013). Deformation analysis of elliptical cross-section spiral equal channel extrusion technique. *Rare Metal Materials and Engineering, 42*(4), 679–683. https://doi.org/10.1016/S1875-5372(13)60055-7

30. Wang, C., Li, F., & Liu, J. (2018). Deformational features and microstructure evolution of copper fabricated by a single pass of the elliptical cross-section spiral equal-channel extrusion (ECSEE) process. *Journal of Materials Engineering and Performance, 27*(6), 2967–2977. https://doi.org/10.1007/s11665-018-3265-2

31. Zhou, T., et al. (2024). Excellent strength-ductility synergy properties of Mg–Sn–Zn–Zr alloy mediated by a novel differential thermal ECAP (DT-ECAP). *Materials Science and Engineering: A, 899*, 146469. https://doi.org/10.1016/j.msea.2024.146469